Received: 7 November 2021 | Revised: 12 February 2022 | Accepted: 30 March 2022

DOI: 10.1002/mp.15660

RESEARCH ARTICLE

MEDICAL PHYSICS

Experimental investigation of dynamic real-time rotation-including dose reconstruction during prostate tracking radiotherapy

Casper Gammelmark Muurholm[1] | **Thomas Ravkilde**[2] | **Robin De Roover**[3,4] | **Simon Skouboe**[5] | **Rune Hansen**[2] | **Wouter Crijns**[3,4] | **Tom Depuydt**[3,4] | **Per R. Poulsen**[1,5]

[1]Department of Oncology, Aarhus University Hospital, Aarhus, Denmark

[2]Department of Medical Physics, Aarhus University Hospital, Aarhus, Denmark

[3]Department of Oncology, KU Leuven, Leuven, Belgium

[4]Department of Radiation Oncology, University Hospitals Leuven, Leuven, Belgium

[5]Danish Center for Particle Therapy, Aarhus University Hospital, Aarhus, Denmark

Correspondence
Casper Gammelmark Muurholm, Danish Center for Particle Therapy, Aarhus University Hospital, Palle Juul-Jensens Boulevard 99, 8200 Aarhus N, Denmark.
Email: casmuu@rm.dk

Funding information
DCCC Radiotherapy (the Danish National Research Center for Radiotherapy); Kræftens Bekæmpelse (DCS). Grant number: R191-A11526; Kom op tegen Kanker (Stand up to Cancer) grant from the Flemish Cancer Society; Varian Medical Systems

Abstract

Background: Hypofractionation in prostate radiotherapy is of increasing interest. Steep dose gradients and a large weight on each individual fraction emphasize the need for motion management. Real-time motion management techniques such as multileaf collimator (MLC) tracking or couch tracking typically adjust for translational motion while rotations remain uncompensated with unknown dosimetric impact.

Purpose: The purpose of this study is to demonstrate and validate dynamic real-time rotation-including dose reconstruction during radiotherapy experiments with and without MLC and couch tracking.

Methods: Real-time dose reconstruction was performed using the in-house developed software DoseTracker. DoseTracker receives streamed target positions and accelerator parameters during treatment delivery and uses a pencil beam algorithm with water density assumption to reconstruct the dose in a moving target. DoseTracker's ability to reconstruct motion-induced dose errors in a dynamically rotating and translating target was investigated during three different scenarios: (1) no motion compensation and translational motion correction with (2) MLC tracking and (3) couch tracking.

In each scenario, dose reconstruction was performed online and in real time during delivery of two dual-arc volumetric-modulated arc therapy prostate plans with a prescribed fraction dose of 7 Gy to the prostate and simultaneous intraprostatic lesion boosts with doses of at least 8 Gy, but up to 10 Gy as long as the organs at risk dose constraints were fulfilled. The plans were delivered to a pelvis phantom that replicated three patient-measured motion traces using a rotational insert with 21 layers of EBT3 film spaced 2.5 mm apart. DoseTracker repeatedly calculated the actual motion-including dose increment and the planned static dose increment since the last calculation in 84 500 points in the film stack. The experiments were performed with a TrueBeam accelerator with MLC and couch tracking based on electromagnetic transponders embedded in the film stack.

The motion-induced dose error was quantified as the difference between the final cumulative dose with motion and without motion using the 2D 2%/2 mm γ-failure rate and the difference in dose to 95% of the clinical target volume (CTV $\Delta D_{95\%}$) and the gross target volume (GTV $\Delta D_{95\%}$) as well as the

difference in dose to 0.1 cm^3 of the urethra, bladder, and rectum ($\Delta D_{0.1CC}$). The motion-induced errors were compared between dose reconstructions and film measurements.

Results: The dose was reconstructed in all calculation points at a mean frequency of 4.7 Hz. The root-mean-square difference between real-time reconstructed and film-measured motion-induced errors was 3.1%-points (γ-failure rate), 0.13 Gy (CTV $\Delta D_{95\%}$), 0.23 Gy (GTV $\Delta D_{95\%}$), 0.19 Gy (urethra $\Delta D_{0.1CC}$), 0.09 Gy (bladder $\Delta D_{0.1CC}$), and 0.07 Gy (rectum $\Delta D_{0.1CC}$).

Conclusions: In a series of phantom experiments, online real-time rotation-including dose reconstruction was performed for the first time. The calculated motion-induced errors agreed well with film measurements. The dose reconstruction provides a valuable tool for monitoring dose delivery and investigating the efficacy of advanced motion-compensation techniques in the presence of translational and rotational motion.

KEYWORDS
couch tracking, intrafraction motion management, MLC tracking, prostate cancer, real-time online dose reconstruction, six degree of freedom motion

1 | INTRODUCTION

In recent years, there has been an increasing interest in the use of stereotactic body radiotherapy (SBRT) for prostate cancer.[1,2] With fewer fractions in the treatment course, there is an increased need for motion management and quality assurance (QA), especially for extreme hypofractionation where each fraction represents a large part of the total dose delivery[3–5] and steep dose gradients are used to protect nearby organs at risk (OAR).[6]

Intrafraction translational motion of the prostate is often quite small, but it can occasionally be up to 15 mm.[7] Furthermore, intrafraction prostate rotations can be substantial with studies reporting rotations about the left–right axis that were larger than 5° for more than a third of the measurement time[8] and occasionally near[8] or exceeding 20°.[9] Methods for intrafraction prostate motion correction on a conventional radiotherapy accelerator include beam gate-off followed by couch corrections[5,10–13] and real-time tumor tracking where either the multileaf collimator (MLC)[14–19] or the couch[19–21] is moved to ensure that the prostate remains aligned with the beam as planned. These methods usually adjust to translational motion only[17,18] while geometrical errors due to prostate rotations are uncorrected.

The dosimetric effect of prostate motion may be investigated by motion-including dose reconstruction. Several studies conducted motion-including dose reconstructions that accounted for the effects of dynamic translational motion. This includes offline studies where the dose reconstruction was performed after treatment delivery[4,5,14,15,22] and online studies where the dose reconstruction was performed during actual treatment delivery.[23–27] The online dose reconstruction studies include treatments of "air" in lieu of a patient using simulated motion monitoring,[23–25] treatments of a moving dosimeter using optical motion monitoring,[26] and treatments of patients using combined optical and image-based motion monitoring.[27]

Rotation-including dose reconstruction studies have so far only been performed offline after treatment delivery. Several studies investigated the effects of static prostate rotations and thus neglected interplay effects,[24,28–31] while three studies investigated the effects of dynamic prostate rotations.[32–34] One study investigated the effects of translational and rotational prostate motion during MR-linac treatments acquired with a temporal resolution of 8.5 or 16.9 s.[34] A second study investigated the effects of dynamic prostate rotations in an anthropomorphic phantom by scripting in a commercial treatment planning system (TPS). The study revealed large dose differences between dynamic and constant rotations emphasizing the need for including dynamic rotations when investigating the impact of rotational motion.[33] However, the TPS dose reconstruction method is not suited for real-time use and also not compatible with real-time MLC aperture adaptation approaches such as MLC tracking. A third study performed dose reconstruction for simulated dynamic prostate rotations using the software DoseTracker,[26] which was developed for real-time motion-including dose reconstruction and extended with the capability to include rotational motion.[32] Dose reconstruction for a single simulated prostate volumetric-modulated arc therapy (VMAT) fraction indicated similarly large dose differences between dynamic and static prostate rotations.[32] However, the dose reconstruction was only performed offline and it was not validated by experiments or independent rotation-including dose calculations. If performed in real time and online during actual treatment delivery the dose reconstruction

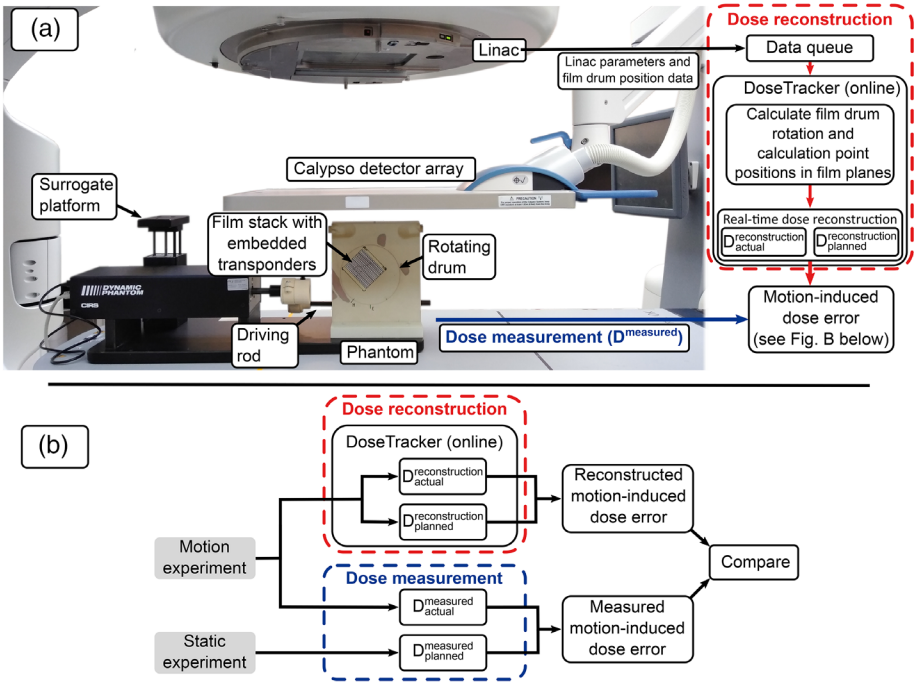

FIGURE 1 (a) Experimental setup using a pelvis phantom with a radiochromic film stack placed in a rotating drum. Calypso transponders embedded in the film stack allowed multileaf collimator (MLC) and couch tracking. A live stream of linac parameters and the drum rotation were streamed to the dose reconstruction software DoseTracker. The contralateral side of the pelvis phantom, present during experiments, was left out in the figure to enable visualization of the film stack. (b) Post-treatment, the motion-induced dose errors were compared between the dose reconstructions and film measurements

would be of great value for real-time QA providing the ability to evaluate the dosimetric quality of an ongoing treatment and take action in case of unacceptable doses. Such QA seems highly needed considering the current developments toward extreme hypofractionation in single-fraction prostate SBRT protocols,[35] where offline post-treatment dose reconstruction would be too late to catch and correct dose errors.

The aim of the current study is to demonstrate real-time online rotation-including dose reconstruction using DoseTracker, and to validate the reconstructed motion-induced dose errors against film dosimetry in a series of tracking and non-tracking phantom experiments. When combined with real-time six degree of freedom (6DoF) motion monitoring,[36] the dose reconstructions can greatly improve QA of the actually delivered dose to the patient.

2 | METHODS AND MATERIALS

2.1 | Treatment planning and delivery

An anthropomorphic pelvis phantom with dynamic rotation capabilities (CIRS, Norfolk, VA, USA) was used for experimental validation of real-time rotation-including dose reconstruction (Figure 1a). The experimental setup has been described previously.[37]

In brief, two 6 MV dual-arc prostate SBRT plans with focal boosts were made for the pelvis phantom using dose prescriptions from the hypo-FLAME trial.[38] Anatomical structures from two prostate patients treated within the FLAME trial[39] were rigidly mapped onto the phantom. The prostate gland was delineated as the clinical target volume (CTV), while magnetic resonance imaging (MRI) visible intraprostatic lesions were delineated as focal boost volumes (gross tumor volume (GTV)). A 4 mm isotropic margin around the GTV was included in the CTV. The CTV-to-PTV margin was 4 mm. The urethra, bladder, and rectum were delineated as OARs. The prescribed CTV dose was 35 Gy in five fractions. The focal boost to the GTV aimed to deliver a minimal total dose of 40 Gy and up to 50 Gy as long as the OAR dose constraints were fulfilled.

The treatment plans were delivered to the pelvis phantom using a TrueBeam linear accelerator (Varian Medical Systems, Palo Alto, CA, USA). The delivered dose was measured with a film stack consisting of 21 layers of radiochromic film (GafChromic EBT3, Ashland Specialty Ingredients, Wayne, NJ, USA) placed in a rotatable drum (Figure 1a). The film layers were 6.3×6.3 cm^2 and spaced 2.5 mm apart. The CTV, GTV, and urethra structures were fully included in the film stack while the rectum and bladder structures extended beyond the stack. Three Calypso electromagnetic transponders embedded in the film stack allowed real-time adaptation to

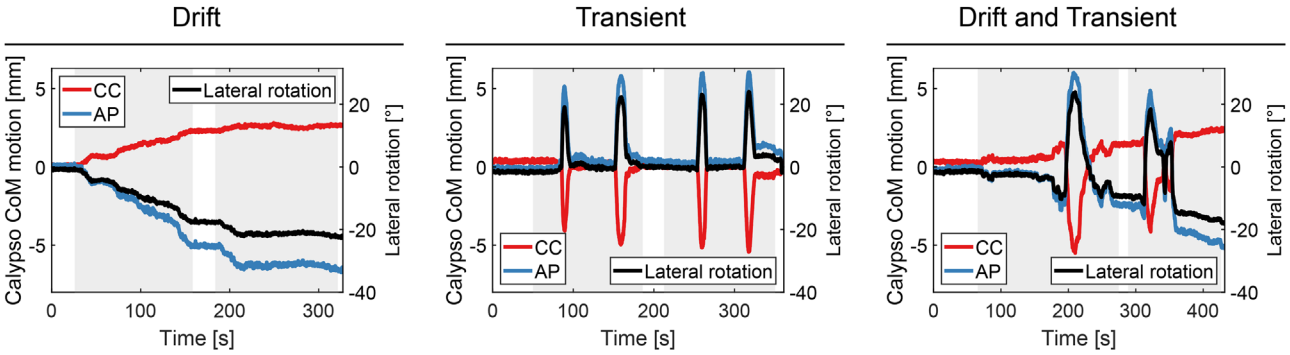

FIGURE 2 The three motion trajectories used in experiments. Left vertical axis: measured center of mass (CoM) position of the three transponders in the cranio-caudal (CC) and anterior–posterior (AP) directions during an experiment with multileaf collimator (MLC) tracking. Right vertical axis: calculated lateral rotation of the drum containing the film stack

3D translations of the center of mass (CoM) of the three transponders by couch and MLC tracking.[19] For technical reasons, the non-tracking motion experiments used an optical marker block (RPM, Varian Medical Systems) on a surrogate platform that moved in synchrony with the film drum rotation instead of the Calypso system for real-time determination of the film stack rotation (Figure 1a). The experiments using the Calypso system and RPM monitoring were completed on different days.

The phantom reproduced three patient-measured prostate motion trajectories[7] by programmed rotation of the film drum around the lateral axis. The rotation resulted in translation of the transponder CoM in the cranio-caudal (CC) and anterior–posterior (AP) directions (Figure 2). For both treatment plans, the apex of the prostate structure was close to the rotation point in the center of the film drum. Examples of measurements of the three motion trajectories during these experiments are shown in Figure 2 where they are described as *drift motion*, *transient* motion, and *drift and transient motion*. The illustrated CC and AP motion were measured by the Calypso system while the lateral rotation was calculated using the relationship between the transponder CoM position and the drum rotation.

Each plan was delivered to the phantom without motion and with the three motion trajectories. The motion experiments were performed with no motion compensation, with MLC tracking and with couch tracking. In total, 18 motion experiments (2 plans × 3 trajectories × 3 motion mitigation methods) and four static experiments (2 plans × 2 experimental sessions) were performed.

2.2 | Real-time online 6DoF dose reconstruction

The real-time rotation-including dose reconstruction was implemented as an upgrade to the motion-including dose reconstruction software DoseTracker. DoseTracker uses a simplistic non-voxel-based pencil beam algorithm to calculate the dose to a predefined set of movable calculation points assuming water density inside the patient volume. In this study, DoseTracker was upgraded to allow dynamic rotations in addition to translations of the calculation points. Consider a calculation point with a planned position $r = (x, y, z)$. After rotating and translating, the point is moved to r' given by

$$r' = R(r - r_0) + r_0 + r_{\mathbf{T}}. \quad (1)$$

Here, r_0 is the center of rotation, $r_{\mathbf{T}}$ is the vector defining the translation, and R is the rotation matrix given by

$$R = R_x R_y R_z = \begin{pmatrix} \cos(\beta)\cos(\gamma) & -\cos(\beta)\sin(\gamma) & \sin(\beta) \\ \cos(\alpha)\sin(\gamma) + \sin(\alpha)\sin(\beta)\cos(\gamma) & \cos(\alpha)\cos(\gamma) - \sin(\alpha)\sin(\beta)\sin(\gamma) & -\sin(\alpha)\cos(\beta) \\ \sin(\alpha)\sin(\gamma) - \cos(\alpha)\sin(\beta)\cos(\gamma) & \sin(\alpha)\cos(\gamma) + \cos(\alpha)\sin(\beta)\sin(\gamma) & \cos(\alpha)\cos(\beta) \end{pmatrix}, \quad (2)$$

where α, β, and γ are rotation angles about the x-axis (right to left), y-axis (caudal to cranial), and z-axis (posterior to anterior), respectively.

DoseTracker was initialized by loading the relevant DICOM files (RT Structure Set, RT Plan) before treatment start. The calculation points were established to match the film plane geometry with dose reconstruction being performed in the 20 inter-film planes interlaced midway between the 21 film planes. The planes were spaced 2.5 mm apart. In each plane, dose reconstruction was performed with a resolution of 1×1 mm^2. The resulting matrix had a size of $65 \times 65 \times 20$ which resulted in 84 500 calculation points.

During the experiments, an in-house modified version of the frame grabber software iTools Capture (Varian Medical Systems) received a stream of non-exposed mega-voltage images, extracted relevant linac parameters and film drum position data from the image headers, and broadcasted these data to DoseTracker as User Datagram Protocol (UDP) messages (Figure 1a). DoseTracker, running on a different computer, received the UDP messages and added the data to a data queue in a continuous loop. Another continuous loop emptied the data queue and calculated the dose increment in all calculation points. If data covering more than 500 ms had accumulated in the data queue, the queue was emptied in portions of maximum 500 ms to prevent averaging over longer time intervals. DoseTracker calculated the dose in two ways serially. The first calculation was the actual dose, that is the motion-including dose. It was based on the received data from the machine such as MLC positions, couch position, and monitor units delivered as well as the film drum position. The second calculation was the planned dose. It used the delivered number of monitor units to look up the machine parameters in the DICOM-RT plan and calculated the dose with a static target. The dose reconstruction was performed on a computer with an Intel Core i7-8700 CPU.

The film drum position data received by DoseTracker (Figure 1a) was either the surrogate platform position (non-tracking experiments) or the Calypso transponder CoM position (tracking experiments). In non-tracking experiments, DoseTracker calculated the film drum rotation using the relationship between platform position and drum rotation. In tracking experiments, DoseTracker used the transponder CoM position relative to the rotation center in the middle of the drum. For MLC tracking, the drum center was fixed in room coordinates. For couch tracking, it changed with the shifting couch positions, but it could be determined from the difference between the initial couch position and the shifted couch position, which was streamed along with the other linac parameters. After calculation of the drum rotation, the positions of all calculation points in the film stack were determined using Equations (1) and (2).

2.3 | Film analysis and comparison of motion-induced errors

The film doses were read out using an Epson 12000XL scanner (Seiko Epson Corporation, Japan) with a resolution of 0.169 mm. The transmittance was converted to dose using the calibration method established by Crijns et al.[40] In addition, the three color channels from the scan were used for multichannel nonuniformity correction.[41] A reference film was homogenously irradiated to 7 Gy after each irradiation and then included during the scanning procedure to help account for scan-to-scan and film-to-film response and linac output variability.[42] To reduce noise, the 21 film planes were converted to 20 dose planes situated between the film layers, by letting each dose voxel be the average of the film pixel above and below. This part of the dose read-out has been previously described in more detail.[37] To further reduce the noise, an 11 × 11 pixel median and subsequently an 11 × 11 pixel Wiener filter were applied.

After extraction of film doses, the motion-induced dosimetric errors were quantified by comparing the motion doses with corresponding static doses. The motion-induced errors were then compared between the real-time dose reconstruction and the film doses (Figure 1b).

For film dosimetry, the effects of motion were calculated by comparing the motion experiments with a static experiment performed on the same date. For the reconstructed dose, the comparison was between the motion-including dose and the planned dose, which were both calculated in the real-time dose reconstruction loop. The motion-induced errors were quantified as 2D γ-failure rates and changes in dose–volume histogram (DVH) parameters. The γ-failure rate was calculated in Matlab R2019b (Mathworks, Natick, MA, USA) using both a 2% (global)/2 mm and a 3% (global)/2 mm criterion for all points with doses above 10% of the global maximum in the static dose. The DVHs were constructed by first importing the dose matrices and DICOM-RT structure sets into 3D Slicer[43] (www.slicer.org, version 4.10.2). Using 3D Slicer, the GTV, CTV, rectum, urethra, bladder, and the active volume (volume in which the dose measurements were valid) were used to generate Boolean masks with a resolution of 0.1×0.1 mm^2. The dose matrices were similarly resampled to a resolution of 0.1×0.1 mm^2 using a B-spline in 3D Slicer. The upsampled matrices were exported from 3D Slicer and the final DVHs were calculated using Matlab. For the CTV and GTV, the parameter that was compared between film dose and reconstructed dose was the motion-induced change in minimum dose to the 95% of the volume that received the highest dose ($\Delta D_{95\%}$). For the urethra, bladder, and rectum, the comparison was on the motion-induced change in minimum dose to the 0.1 cm^3 that received the highest dose ($\Delta D_{0.1\mathrm{CC}}$).

Besides comparisons of the final cumulative dose, time-resolved data from DoseTracker were analyzed for one experiment with the *drift motion* trajectory to show the benefits of real-time online dose reconstruction. For all experiments, the time between UDP messages as well as the real-time dose reconstruction speed were analyzed using the mean and standard deviation. Additionally, the maximum dose calculation time was reported.

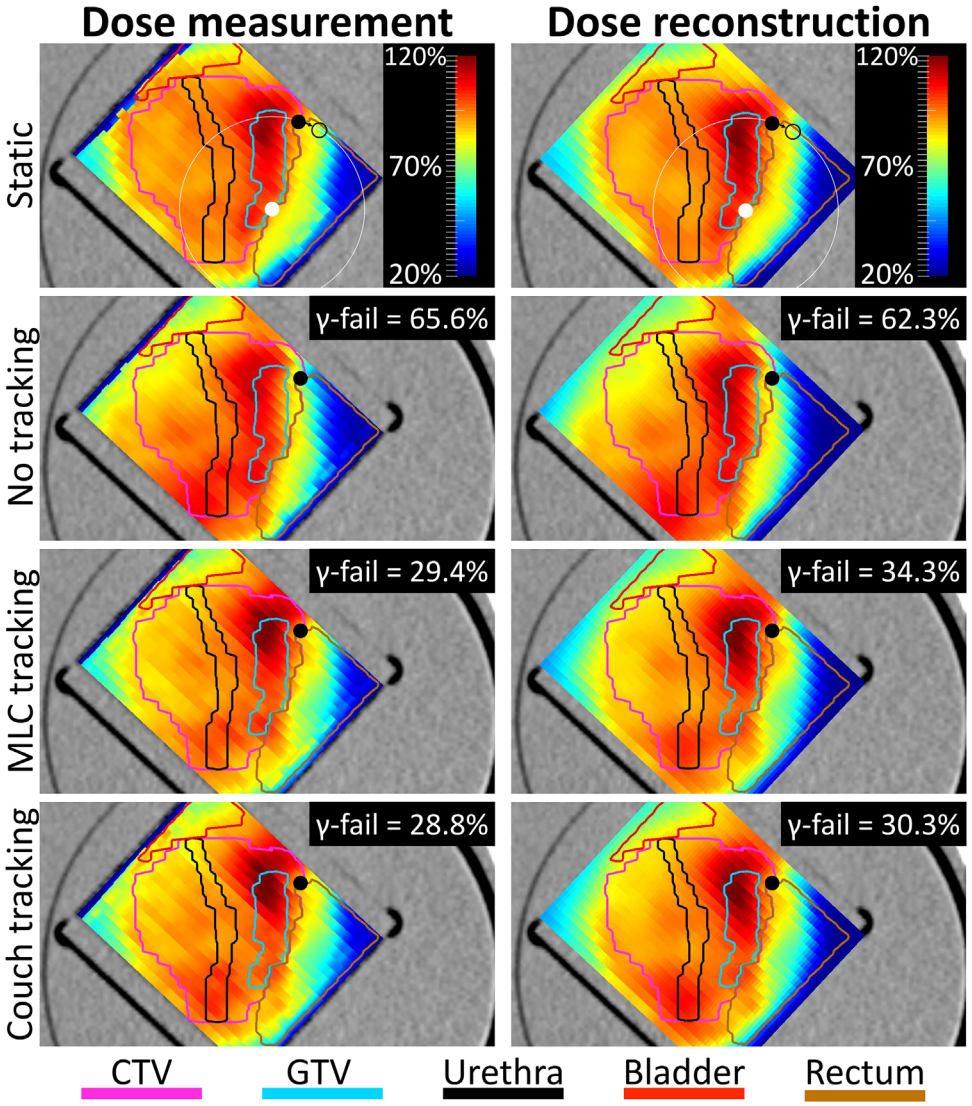

FIGURE 3 Measured and real-time reconstructed dose distributions in the sagittal plane for experiments without motion (top) and with the drift motion trajectory. The shown doses are normalized to the planned (measured or reconstructed) mean clinical target volume (CTV) dose for easier comparison. The colored outlines show the target and organ at risk structures investigated in this study. The rectum and bladder are cropped to the volume where the film stack allows accurate measurement. The motion-induced 2%/2 mm γ-failure rates are indicated for each motion case with the static dose as reference. The solid black dot shows the point which was used for the time-resolved analysis in Figure 4. In the top row, the mean lateral rotation of the drift motion trajectory (14°) is shown as the solid black dot moving to the open black dot. The white dot is the center of rotation for the drum in the phantom

3 | RESULTS

The mean (standard deviation) time between UDP messages was 48.1 ms (10.4 ms) corresponding to a transmission rate of 20.8 Hz. The real-time reconstructions of both the actual and the planned dose in 84 500 calculation points took 212 ms (70 ms). The real-time dose reconstruction duration had a maximum of 2.6 s and exceeded 500 ms in 23 out of 28 154 cases. In these cases, the subsequent dose calculations were queued and performed with a latency while ensuring a max time resolution of 500 ms. Figure 3 shows examples of the dose in the sagittal plane for the static experiment and experiments using the *drift motion* trajectory with and without tracking. In the motion experiments, the point marked with the solid black dot at the edge of the CTV moved to a mean position slightly outside the CTV as marked with an open black dot in the top row of the figure. Consequently, this point received less dose than planned without tracking (second row). In general, the experiment without tracking resulted in a rotated and shifted dose distribution, slightly reducing the dose coverage of both the CTV and GTV. With tracking, the translation was compensated for, while the rotation effects remained. This improved the CTV coverage since the CTV was relatively spherical. The focal boost dose,

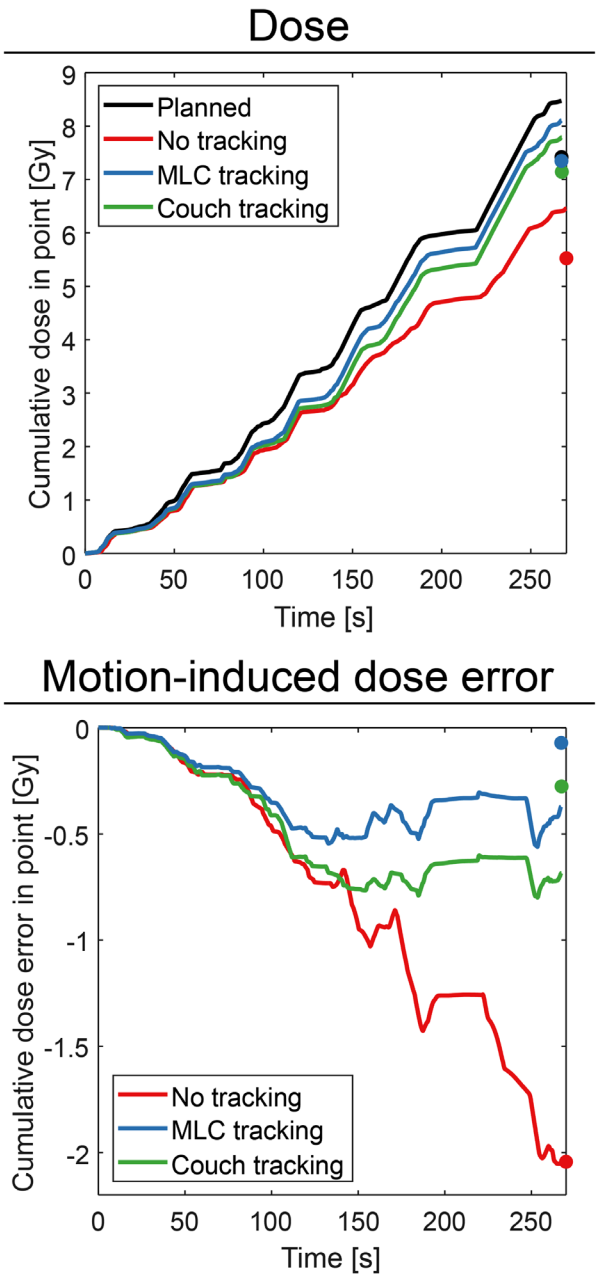

FIGURE 4 Real-time reconstructed dose (top) and motion-induced dose error (bottom) during experiments with drift motion shown as a function of time in the point marked with a solid black dot in Figure 3. The colored circles in the right side of the figures show the film-measured final dose and motion-induced dose error in the point

however, covered less of the intended GTV region and gave high doses outside the intraprostatic lesion. Similar consequences were seen for the OARs, for example giving unintended hotspots in the urethra. In general, the dose reconstruction reproduced these features well and resulted in motion-induced γ-failure rates in good agreement with the film doses as seen in Figure 3.

Figure 4 presents the time-resolved dose and dose error in the point marked with the solid black dot in Figure 3. While the final cumulative reconstructed dose in this point was 0.9–1.1 Gy higher than the film-measured dose (Figure 4, top), the reconstructed motion-induced dose error showed better agreement (Figure 4, bottom). DoseTracker showed motion-induced dose errors in the point of −2.03 Gy (no tracking), −0.37 Gy (MLC tracking), and −0.68 Gy (couch tracking) while the film dosimetry showed errors of −2.04 Gy (no tracking), −0.07 Gy (MLC tracking), and −0.28 Gy (couch tracking) in the point (Figure 4, bottom).

The motion-induced γ-failure rate was highly dependent on the motion trajectory (Figure 5). The largest γ-failure rate occurred for the two experiments without motion compensation while applying the drift motion trajectory, which had a persistent rotation of around -22° for most of the second VMAT arc (Figure 2). Compared to film measurements, the reconstructed motion-induced γ-failure rate had root-mean-square errors (RMSE) of 3.1%-points (2% (global)/2 mm) and 2.8%-points (3% (global)/2 mm). The investigated DVH parameters for delineated structures had RMSE of 0.13 Gy (CTV $\Delta D_{95\%}$), 0.23 Gy (GTV $\Delta D_{95\%}$), 0.19 Gy (urethra $\Delta D_{0.1CC}$), 0.09 Gy (bladder $\Delta D_{0.1CC}$), and 0.07 Gy (rectum $\Delta D_{0.1CC}$).

4 | DISCUSSION

In this study, real-time 6DoF motion-including dose reconstruction was developed and demonstrated online in phantom experiments for the first time. Real-time reconstruction of OAR doses was also demonstrated for the first time, albeit with OARs rigidly moving with the prostate in the experimental setup. While the reconstructed absolute doses deviated somewhat from film-measured doses (Figure 4, top), the reconstructed motion-induced dose errors were in excellent agreement with film dosimetry (Figure 5).

The results showed that while tracking improves the dose delivery there are still uncorrected residual dosimetric errors, presumably partly because the tracking only adjusts for translational motion. It would be of great interest to investigate tracking systems which can account for rotations. As an example, MLC tracking can potentially take into account in-plane rotations,[44] but this is not standard on MLC tracking systems and not available in our clinic.

Clinical implementation of the 6DoF motion-including dose reconstruction seems feasible for several reasons. First, the required real-time 6DoF motion monitoring has been implemented for prostate using kilovoltage intrafraction monitoring.[36] Second, the 5 Hz dose reconstruction frequency (0.2 s reconstruction time) should be sufficiently fast to capture the dynamics of both prostate motion and accelerator motion as indicated by the good agreement with film dosimetry. Prostate motion within a 0.2 s time interval is generally very small and the

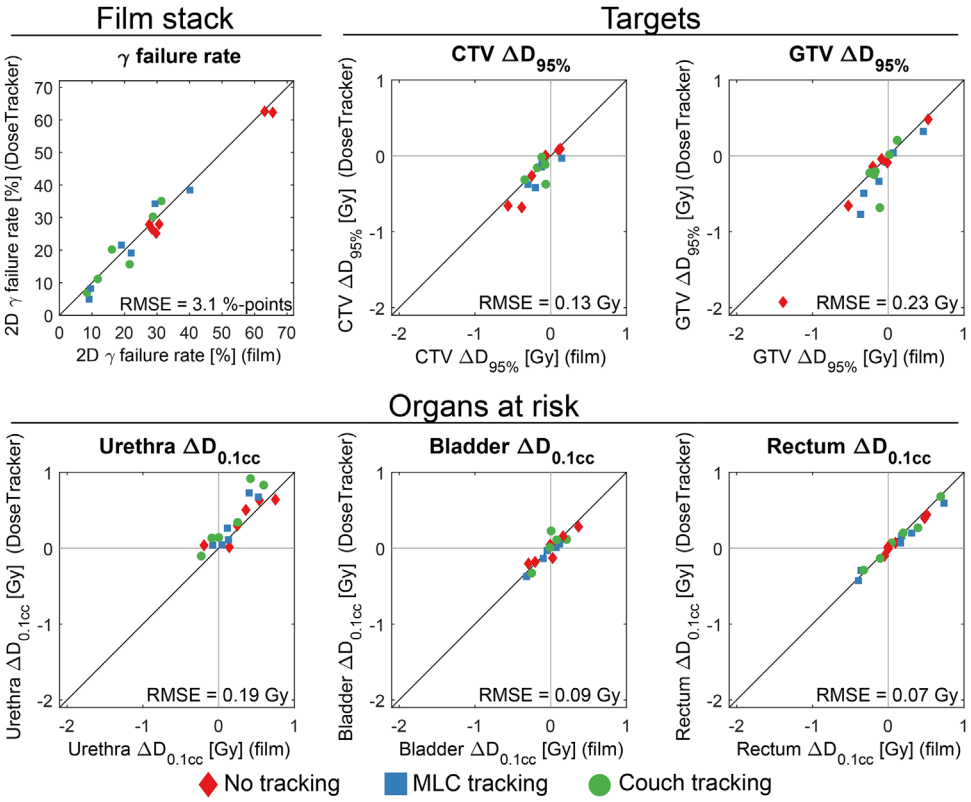

FIGURE 5 Real-time reconstructed versus film-measured differences between motion doses and static doses for all experiments, quantified as the 2%/2 mm γ-failure rate (top left), target $\Delta D_{95\%}$ (top middle/right), and organ at risk $\Delta D_{0.1CC}$ (bottom). The numbers indicate the root-mean-square error (RMSE) of the dose reconstructions when compared to film measurements

VMAT gantry rotation in 0.2 s is limited to 1.2°. Third, online real-time dose reconstruction with DoseTracker has already been demonstrated clinically for liver SBRT although only for translational tumor motion.[27] Finally, real-time calculation of DVH parameters in DoseTracker was recently demonstrated in a simulation study[45] making these important parameters for decision making available during treatment delivery.

In this study, the dose to the film volume which included the CTV and urethra, but only partial rectum and bladder volumes was calculated. A previous study[46] investigated the relationship between calculation time and the number of calculation points for DoseTracker. From this relationship, we would expect a calculation time of approximately 238 ms in the current study, while a value of 212 ms was found. The difference can be attributed to a different CPU which is faster even when including rotational motion. The estimated calculation time for the full volumes of the investigated structures (26% and 38% additional calculation points for the two cases) is up to 310 ms, which suggests that DoseTracker would be able to include the full OAR volumes without loss of real-time effectiveness.

The main objective of the study was to compare the real-time reconstructed motion-induced dose errors with the film-measured motion-induced errors. While it would also be interesting to compare absolute doses, DoseTracker's simplified algorithm results in errors in the absolute dose,[46] making a direct comparison with the film measurement difficult. Due to the absolute dose errors being present in both the motion-including and static calculation, DoseTracker can still provide valuable data when calculating the motion-induced dose difference since the absolute dose errors effectively cancel out.

Only few previous studies have demonstrated dose reconstruction accounting for dynamic translations and rotations. Kontaxis et al.[34] did dynamic 6DoF motion-including dose reconstruction using cine-MR images and treatment log files with a time resolution of 8.5 or 16.9 s. The prostate motion was acquired using soft-tissue rigid registration, while the body contour and bony anatomy were kept fixed for each fraction. The study included five prostate patients undergoing 20 fractions of 3.1 Gy each. The full treatment dose accumulation showed adequate dose delivery for all patients, but several fractions with large motion led the authors to conclude that dose reconstruction and intrafraction adaptations are essential as hypofractionation use increases for prostate radiotherapy. Based on the non-tracking experiments in the current study, Skouboe et al.[33] performed 6DoF motion-including dose

reconstruction using application programming interface scripting in a commercial TPS. The dose reconstruction was performed by moving the calculation points in a time-resolved version of the planned dose matrix while cumulating the dose in the moving points under the assumption of shift invariant dose distributions. A key finding of the study was that assumption of a constant mean prostate rotation was insufficient when calculating the dosimetric effects of dynamic prostate rotations.[33] This is in agreement with a simulation study by Muurholm et al.[32] Although the method applied by Skouboe et al.[33] potentially could be used in real time, it cannot be used for real-time online MLC tracking where the MLC aperture deviates from the planned aperture. Real-time dose reconstruction during MLC tracking has, however, been shown in phantom simulations with translational liver motion by Ravkilde et al. who used DoseTracker, and for prostate motion by Fast et al.[24] who used dose influence matrices to allow real-time handling of differences between planned and the actual MLC apertures.

While this study extended the online real-time dose reconstruction of DoseTracker from translational motion to 6DoF motion, a natural next level in motion complexity would be to include deformations. It should be noted that the dose calculation time of DoseTracker mainly depends on the number of calculation points while the type of motion (translation, rotation, deformation) only has a minor impact on the calculation speed. The main challenge would therefore be to obtain reliable deformation information in real time. Deformations can happen due to, for example prostate swelling, intrafractional bladder filling and rectal flatulence which cannot be captured fully using implanted fiducial markers or transponders. However, these complex movements may be captured in clinical practice using linacs equipped with MRI (MR-linac).[47] In such a case, DoseTracker could perform deformation-including real-time dose reconstruction online for both targets and OARs for improved QA during SBRT treatments.

Besides the real-time online capabilities of DoseTracker, the dose reconstructions with dynamic motion may be used for comprehensive motion-including dose analysis. Film experiments are very time consuming and complex. Dose reconstruction allows both offline investigations of the dosimetric impact of complex motion observed during actual treatments and investigation of the motion robustness of a given treatment strategy by simulations that combine a large number of treatment plans and motion trajectories.

5 | CONCLUSION

In a series of phantom experiments, online real-time rotation-including dose reconstruction was performed for the first time. The reconstructed motion-induced dose errors showed good agreement with the film doses, showing promise for clinical implementation and applicability for investigation of complex motion effects during radiotherapy treatments and the efficacy of real-time motion adaptation techniques.

ACKNOWLEDGMENTS

This work was supported by DCCC Radiotherapy (the Danish National Research Center for Radiotherapy), Kom op tegen Kanker (Stand up to Cancer), and Varian Medical Systems.

CONFLICT OF INTEREST

This work was supported by Varian Medical Systems by in-kind loan of iTools Tracking and iTools Capture software.

REFERENCES

1. Draulans C, De Roover R, van derHeide UA, et al. Stereotactic body radiation therapy with optional focal lesion ablative microboost in prostate cancer: topical review and multicenter consensus. *Radiother Oncol*. 2019;140:131-142. http://doi.org/10.1016/j.radonc.2019.06.023
2. Mahase SS, D'Angelo D, Kang J, Hu JC, Barbieri CE, Nagar H. Trends in the use of stereotactic body radiotherapy for treatment of prostate cancer in the United States. *JAMA Netw Open*. 2020;3(2):e1920471. http://doi.org/10.1001/jamanetworkopen.2019.20471
3. Ghadjar P, Fiorino C, Munck af Rosenschöld P, Pinkawa M, Zilli T, van derHeide UA. ESTRO ACROP consensus guideline on the use of image guided radiation therapy for localized prostate cancer. *Radiother Oncol*. 2019;141:5-13. http://doi.org/10.1016/j.radonc.2019.08.027
4. Vanhanen A, Poulsen P, Kapanen M. Dosimetric effect of intrafraction motion and different localization strategies in prostate SBRT. *Phys Med*. 2020;75:58-68. http://doi.org/10.1016/j.ejmp.2020.06.010
5. Jaccard M, Ehrbar S, Miralbell R, et al. Single-fraction prostate stereotactic body radiotherapy: dose reconstruction with electromagnetic intrafraction motion tracking. *Radiother Oncol*. 2021;156:145-152. http://doi.org/10.1016/j.radonc.2020.12.013
6. Benedict SH, Yenice KM, Followill D, et al. Stereotactic body radiation therapy: the report of AAPM task group 101. *Med Phys*. 2010;37(8):4078-4101. http://doi.org/10.1118/1.3438081
7. Langen KM, Willoughby TR, Meeks SL, et al. Observations on real-time prostate gland motion using electromagnetic tracking. *Int J Radiat Oncol*. 2008;71(4):1084-1090. http://doi.org/10.1016/j.ijrobp.2007.11.054
8. Huang CY, Tehrani JN, Ng JA, Booth J, Keall P. Six degrees-of-freedom prostate and lung tumor motion measurements using kilovoltage intrafraction monitoring. *Int J Radiat Oncol Biol Phys*. 2015;91(2):368-375. http://doi.org/10.1016/j.ijrobp.2014.09.040
9. Deutschmann H, Kametriser G, Steininger P, et al. First clinical release of an online, adaptive, aperture-based image-guided radiotherapy strategy in intensity-modulated radiotherapy to correct for inter- and intrafractional rotations of the prostate. *Int J Radiat Oncol*. 2012;83(5):1624-1632. http://doi.org/10.1016/j.ijrobp.2011.10.009
10. Lovelock DM, Messineo AP, Cox BW, Kollmeier MA, Zelefsky MJ. Continuous monitoring and intrafraction target position correction during treatment improves target coverage for patients undergoing sbrt prostate therapy. *Int J Radiat Oncol Biol Phys*. 2015;91(3):588-594. http://doi.org/10.1016/j.ijrobp.2014.10.049

11. Keall PJ, Ng JA, Juneja P, et al. Real-time 3D image guidance using a standard LINAC: measured motion, accuracy, and precision of the first prospective clinical trial of kilovoltage intrafraction monitoring–guided gating for prostate cancer radiation therapy. *Int J Radiat Oncol*. 2016;94(5):1015-1021. http://doi.org/10.1016/j.ijrobp.2015.10.009
12. Rosario T, van derWeide L, Admiraal M, Piet M, Slotman B, Cuijpers J. Toward planning target volume margin reduction for the prostate using intrafraction motion correction with online kV imaging and automatic detection of implanted gold seeds. *Pract Radiat Oncol*. 2018;8(6):422-428. http://doi.org/10.1016/j.prro.2018.04.008
13. Kisivan K, Antal G, Gulyban A, et al. Triggered imaging with auto beam hold and pre-/posttreatment CBCT during prostate SABR: analysis of time efficiency, target coverage, and normal volume changes. *Pract Radiat Oncol*. 2021;11(2):e210-e218. http://doi.org/10.1016/j.prro.2020.04.014
14. Colvill E, Booth JT, O'Brien RT, et al. Multileaf collimator tracking improves dose delivery for prostate cancer radiation therapy: results of the first clinical trial. *Int J Radiat Oncol Biol Phys*. 2015;92(5):1141-1147. http://doi.org/10.1016/j.ijrobp.2015.04.024
15. Keall PJ, Nguyen DT, O'Brien R, et al. The first clinical implementation of real-time image-guided adaptive radiotherapy using a standard linear accelerator. *Radiother Oncol*. 2018;127(1):6-11. http://doi.org/10.1016/j.radonc.2018.01.001
16. Fast MF, Nill S, Bedford JL, Oelfke U. Dynamic tumor tracking using the Elekta Agility MLC. *Med Phys*. 2014;41(11):111719. http://doi.org/10.1118/1.4899175
17. Keall PJ, Colvill E, O'Brien R, et al. Electromagnetic-guided MLC tracking radiation therapy for prostate cancer patients: prospective clinical trial results. *Int J Radiat Oncol*. 2018;101(2):387-395. http://doi.org/10.1016/j.ijrobp.2018.01.098
18. Chen G, Tai A, Keiper TD, Lim S, Li XA. Technical note: comprehensive performance tests of the first clinical real-time motion tracking and compensation system using MLC and jaws. *Med Phys*. 2020;47(7):2814-2825. http://doi.org/10.1002/mp.14171
19. Hansen R, Ravkilde T, Worm ES, et al. Electromagnetic guided couch and multileaf collimator tracking on a TrueBeam accelerator. *Med Phys*. 2016;43(5):2387-2398
20. D'Souza WD, Naqvi SA, Yu CX. Real-time intra-fraction-motion tracking using the treatment couch: a feasibility study. *Phys Med Biol*. 2005;50(17):4021-4033. http://doi.org/10.1088/0031-9155/50/17/007
21. Ehrbar S, Schmid S, Jöhl A, et al. Validation of dynamic treatment-couch tracking for prostate SBRT. *Med Phys*. 2017;44(6):2466-2477. http://doi.org/10.1002/mp.12236
22. Langen KM, Chauhan B, Siebers JV, Moore J, Kupelian PA. The dosimetric effect of intrafraction prostate motion on step-and-shoot intensity-modulated radiation therapy plans: magnitude, correlation with motion parameters, and comparison with helical tomotherapy plans. *Int J Radiat Oncol*. 2012;84(5):1220-1225. http://doi.org/10.1016/j.ijrobp.2012.01.046
23. Kamerling CP, Fast MF, Ziegenhein P, Menten MJ, Nill S, Oelfke U. Online dose reconstruction for tracked volumetric arc therapy: real-time implementation and offline quality assurance for prostate SBRT. *Med Phys*. 2017;44(11):5997-6007. http://doi.org/10.1002/mp.12522
24. Fast MF, Kamerling CP, Ziegenhein P, et al. Assessment of MLC tracking performance during hypofractionated prostate radiotherapy using real-time dose reconstruction. *Phys Med Biol*. 2016;61(4):1546-1562. http://doi.org/10.1088/0031-9155/61/4/1546
25. Kamerling CP, Fast MF, Ziegenhein P, Menten MJ, Nill S, Oelfke U. Real-time 4D dose reconstruction for tracked dynamic MLC deliveries for lung SBRT. *Med Phys*. 2016;43(11):6072-6081. http://doi.org/10.1118/1.4965045
26. Ravkilde T, Skouboe S, Hansen R, Worm E, Poulsen PR. First online real-time evaluation of motion-induced 4D dose errors during radiotherapy delivery. *Med Phys*. 2018;45(8):3893-3903. http://doi.org/10.1002/mp.13037
27. Skouboe S, Ravkilde T, Bertholet J, et al. First clinical real-time motion-including tumor dose reconstruction during radiotherapy delivery. *Radiother Oncol*. 2019;139:66-71. http://doi.org/10.1016/j.radonc.2019.07.007
28. Amro H, Hamstra DA, Mcshan DL, et al. The dosimetric impact of prostate rotations during electromagnetically guided external-beam radiation therapy. *Int J Radiat Oncol*. 2013;85(1):230-236. http://doi.org/10.1016/j.ijrobp.2012.03.020
29. Wolf J, Nicholls J, Hunter P, Nguyen DT, Keall P, Martin J. Dosimetric impact of intrafraction rotations in stereotactic prostate radiotherapy: a subset analysis of the TROG 15.01 SPARK trial. *Radiother Oncol*. 2019;136:143-147. http://doi.org/10.1016/j.radonc.2019.04.013
30. Rijkhorst E-J, Lakeman A, Nijkamp J, et al. Strategies for online organ motion correction for intensity-modulated radiotherapy of prostate cancer: prostate, rectum, and bladder dose effects. *Int J Radiat Oncol*. 2009;75(4):1254-1260. http://doi.org/10.1016/j.ijrobp.2009.04.034
31. deBoer J, Wolf AL, Szeto YZ, vanHerk M, Sonke J-J. Dynamic collimator angle adjustments during volumetric modulated arc therapy to account for prostate rotations. *Int J Radiat Oncol*. 2015;91(5):1009-1016. http://doi.org/10.1016/j.ijrobp.2014.11.020
32. Muurholm CG, Ravkilde T, Skouboe S, et al. Dose reconstruction including dynamic six-degree of freedom motion during prostate radiotherapy. *J Phys Conf Ser*. 2019;1305:012053. http://doi.org/10.1088/1742-6596/1305/1/012053
33. Skouboe S, De Roover R, Gammelmark Muurholm C, et al. Six degrees of freedom dynamic motion-including dose reconstruction in a commercial treatment planning system. *Med Phys*. 2021;48(3):1427-1435. http://doi.org/10.1002/mp.14707
34. Kontaxis C, deMuinck Keizer DM, Kerkmeijer LGW, et al. Delivered dose quantification in prostate radiotherapy using online 3D cine imaging and treatment log files on a combined 1.5T magnetic resonance imaging and linear accelerator system. *Phys Imaging Radiat Oncol*. 2020;15:23-29. http://doi.org/10.1016/j.phro.2020.06.005
35. Zilli T, Franzese C, Bottero M, et al. Single fraction urethra-sparing prostate cancer SBRT: phase I results of the ONE SHOT trial. *Radiother Oncol*. 2019;139:83-86. http://doi.org/10.1016/j.radonc.2019.07.018
36. Nguyen DT, O'Brien R, Kim JH, et al. The first clinical implementation of a real-time six degree of freedom target tracking system during radiation therapy based on Kilovoltage Intrafraction Monitoring (KIM). *Radiother Oncol*. 2017;123(1):37-42. http://doi.org/10.1016/j.radonc.2017.02.013
37. De Roover R, Hansen R, Crijns W, et al. Dosimetric impact of intrafraction prostate rotation and accuracy of gating, multileaf collimator tracking and couch tracking to manage rotation: an end-to-end validation using volumetric film measurements. *Radiother Oncol*. 2021;156:10-18. http://doi.org/10.1016/j.radonc.2020.11.031
38. Draulans C, van derHeide UA, Haustermans K, et al. Primary endpoint analysis of the multicentre phase II hypo-FLAME trial for intermediate and high risk prostate cancer. *Radiother Oncol*. 2020;147:92-98. http://doi.org/10.1016/j.radonc.2020.03.015
39. Lips IM, van derHeide UA, Haustermans K, et al. Single blind randomized Phase III trial to investigate the benefit of a focal lesion ablative microboost in prostate cancer (FLAME-trial): study protocol for a randomized controlled trial. *Trials*. 2011;12(1):255. http://doi.org/10.1186/1745-6215-12-255
40. Crijns W, Maes F, van derHeide UA, Van den Heuvel F. Calibrating page sized Gafchromic EBT3 films. *Med Phys*. 2013;40(1):012102. http://doi.org/10.1118/1.4771960

41. Micke A, Lewis DF, Yu X. Multichannel film dosimetry with nonuniformity correction. *Med Phys*. 2011;38(5):2523-2534. http://doi.org/10.1118/1.3576105
42. Lewis D, Devic S. Correcting scan-to-scan response variability for a radiochromic film-based reference dosimetry system. *Med Phys*. 2015;42(10):5692-5701. http://doi.org/10.1118/1.4929563
43. Fedorov A, Beichel R, Kalpathy-Cramer J, et al. 3D Slicer as an image computing platform for the quantitative imaging network. *Magn Reson Imaging*. 2012;30(9):1323-1341. http://doi.org/10.1016/j.mri.2012.05.001
44. Wu J, Ruan D, Cho B, et al. Electromagnetic detection and real-time DMLC adaptation to target rotation during radiotherapy. *Int J Radiat Oncol*. 2012;82(3):e545-e553. http://doi.org/10.1016/j.ijrobp.2011.06.1958
45. Muurholm CG, Ravkilde T, Skouboe S, et al. Real-time dose-guidance in radiotherapy: proof of principle. *Radiother Oncol*. 2021;164:175-182. http://doi.org/10.1016/j.radonc.2021.09.024
46. Skouboe S, Poulsen PR, Muurholm CG, et al. Simulated real-time dose reconstruction for moving tumors in stereotactic liver radiotherapy. *Med Phys*. 2019;46(11):4738-4748. http://doi.org/10.1002/mp.13792
47. Corradini S, Alongi F, Andratschke N, et al. MR-guidance in clinical reality: current treatment challenges and future perspectives. *Radiat Oncol*. 2019;14(1):92. http://doi.org/10.1186/s13014-019-1308-y

How to cite this article: Muurholm CG, Ravkilde T, De Roover R, et al. Experimental investigation of dynamic real-time rotation-including dose reconstruction during prostate tracking radiotherapy. *Med Phys*. 2022;49:3574–3584. https://doi.org/10.1002/mp.15660